Inclusion of image-based in vivo experimental data into the Hill-type muscle model affects the estimation of individual force-sharing strategies during walking.

Raphaël Hamard, François Hug, Nicole Kelp, Romain Feigean, Jeroen Aeles, Taylor Dick

Inclusion of image-based *in-vivo* experimental data into the Hill-type muscle model affects the estimation of individual force-sharing strategies during walking

Raphaël Hamard[1], François Hug*[1,2,3,4], Nicole Y. Kelp[2], Romain Feigean[5], Jeroen Aeles[1], Taylor J. M. Dick[2]

[1] Nantes Université, Movement - Interactions - Performance, MIP, UR 4334, F-44000 Nantes, France
[2] The University of Queensland, School of Biomedical Sciences, Brisbane, Queensland, Australia
[3] Institut Universitaire de France (IUF), Paris, France
[4] Université Côte d'Azur, LAMHESS, Nice, France
[5] Laboratoire de Physiologie et Évaluation Neuromusculaire, Institut de Myologie, Paris, France

Keywords: B-mode ultrasound, Electromyography, Gastrocnemius, MRI, Muscle coordination

Word count: 3494

***Corresponding author:**

Prof. François Hug
Université Côte d'Azur, LAMHESS
Campus STAPS
261 boulevard du Mercantour
06200 Nice (France)
E-mail address: francois.hug@univ-cotedazur.fr
ORCID: 0000-0002-6432-558X

ABSTRACT

The study of muscle coordination requires knowledge of the force produced by individual muscles, which can be estimated using Hill-type models. Predicted forces from Hill-type models are sensitive to the muscle's maximal force-generating capacity (F_{max}), however, to our knowledge, no study has investigated the effect of different F_{max} personalization methods on predicted muscle forces. The aim of this study was to determine the influence of two personalization methods on predicted force-sharing strategies between the human gastrocnemii during walking. Twelve participants performed a walking protocol where we estimated muscle activation using surface electromyography and fascicle length, velocity, and pennation angle using B-mode ultrasound to inform the Hill-type model. F_{max} was determined using either a scaling method or experimental method. The scaling method used anthropometric scaling to determine both muscle volume and fiber length, which were used to estimate the F_{max} of the gastrocnemius medialis and lateralis. The experimental method used muscle volume and fascicle length obtained from magnetic resonance imaging and diffusion tensor imaging, respectively. We found that the scaling and the experimental method predicted similar gastrocnemii force-sharing strategies at the group level (mean over the participants). However, substantial differences between methods in predicted force-sharing strategies was apparent for some participants revealing the limited ability of the scaling method to predict force-sharing strategies at the level of individual participants. Further personalization of muscle models using *in vivo* experimental data from imaging techniques is therefore likely important when using force predictions to inform the diagnosis and management of neurological and orthopedic conditions.

1. INTRODUCTION

Knowledge of the forces that individual muscles produce provides important insights into muscle coordination, and this information can be used to improve the diagnosis and management of many neurological and orthopedic conditions (Hug and Tucker, 2017). However, directly measuring human muscle force requires highly invasive techniques (Finni et al., 1998; Gregor et al., 1987; Komi, 1990), which are not feasible in clinical environments and remain limited in most research settings. To overcome this limitation, muscle models for predicting muscle forces have been developed.

The Hill-type model is the most ubiquitous muscle model in biomechanics (Eq. 1; Zajac, 1989). It takes into account most of the known determinants of muscle force, i.e. the activation, the instantaneous length and velocity of the contracting muscle fibers, and the maximal force-generating capacity (F_{max}). The Hill-type model can be personalized with subject-specific data, such as time-varying muscle activation assessed using surface electromyography (EMG) (Perreault et al., 2003) or time-varying fascicle length, fascicle velocity, and pennation angle recorded using ultrasound imaging (Dick et al., 2017). An important determinant of muscle force is F_{max} (Bujalski et al., 2018; Scovil and Ronsky, 2006), for which the vast majority of studies rely on scaled data using different methods. For example, muscle volume, a determinant of F_{max}, has been personalized through values scaled to the participant's body mass (Dick et al., 2017). Furthermore, optimal muscle fiber length, which is another determinant of F_{max}, is often scaled from generic musculoskeletal models (Millard et al., 2013). An important limitation of these approaches is that they use the same underlying equations to scale all individuals. This conceals the well-described inter-individual variability in the distribution of F_{max} across muscles (Crouzier et al., 2018; Hug et al., 2015).

The aim of this study was to compare two different personalization methods of a Hill-type model to predict human gastrocnemii forces during level and incline walking. The first personalization method, herein referred to as the "scaling method", used anthropometric scaling to determine both muscle volume and muscle fiber length to estimate F_{max} of the gastrocnemius medialis (GM) and lateralis (GL). The second method, named hereafter the "experimental method", used muscle volume and fascicle length obtained from magnetic resonance imaging (MRI) and diffusion tensor imaging (DTI), respectively. We specifically investigated the force-sharing strategy between the two gastrocnemii muscles. Because the scaling method inevitably conceals interindividual variability in the distribution of F_{max}

between the GM and GL, we expected to observe substantial differences between methods when comparing the gastrocnemii force-sharing strategy at the individual level. However, we hypothesized that the two methods would predict similar force-sharing strategies at the group level.

2. MATERIALS AND METHODS

2.1. Participants

Twelve adults with no recent (< 6 months) lower limb pain or injury gave informed written consent to participate in the study (5 females, 7 males, age: 25 ± 3.5 years, body mass: 75.4 ± 16.4 kg, height: 1.71 ± 0.10 m; mean ± standard deviation). This study was approved by the institutional ethics review committee at The University of Queensland (#2013001448).

2.2. Experimental data acquisition

Data were collected over two experimental sessions. The first session consisted of two consecutive scanning sequences of the participant's dominant leg: a T1-weighted MRI scan to determine muscle volume, and a DTI scan to determine muscle fascicle lengths.

For the second session, participants walked on a treadmill (Nautilus Trimline T345, TX, USA) at their preferred walking speed (1.1 ± 0.1 $m.s^{-1}$), which was determined at the beginning of the protocol (Dal et al., 2010). During walking, we recorded surface EMG and B-mode ultrasound of the GM and GL of the dominant leg to measure muscle activation and fascicle behavior, respectively. Foot position was measured using motion capture to identify phases of the gait cycle. Participants walked under two conditions presented in a randomized order: (i) 0% treadmill grade (level walking) and (ii) 10% treadmill grade (incline walking). They performed two trials at each walking condition and repeated each condition a second time, first to record EMG and second to measure fascicle behavior. The EMG and the ultrasound recordings were conducted in separate trials to ensure that the measures were taken on the same mid-region of the muscle belly. Participants also performed three isometric plantar flexion maximal voluntary contractions (MVCs), with 120 s rest between contractions, to determine maximal GM and GL EMG amplitude for EMG normalization. The EMG and ultrasound data have been published elsewhere (Hamard et al., 2021).

2.2.1. MRI

Participants were placed in a 3T MRI scanner (Magnetom Prisma, Siemens, Germany) in a supine position. The dominant foot was secured into a custom-built MRI-compatible foot plate with the hip extended and the ankle positioned in a 90° angle. The dominant knee was positioned in slight flexion (< 5°) by using a foam wedge under the knee. Details on the MRI parameters have been described elsewhere (Pinel et al., 2021). The T1-weighted MRI images were analyzed using a combination of semi-automated (Sashimi V1.1; Bolsterlee, 2020) and

manual segmentation software (ITK-SNAP v3.8.0, NIH, USA). We calculated total muscle volume for the GM and GL as the sum of the volume of all voxels in each muscle (ITK-SNAP v3.8.0, NIH, USA). These muscle volumes were included in the Hill-type model (see 2.3) for the experimental method.

2.2.2. DTI

DTI scans were performed with the same scanner as for the MRI. Detailed information on the DTI parameters, processing and data analyses has been described elsewhere (Aeles et al., 2021). Briefly, the muscle was divided into smaller muscle regions in the local muscle frontal plane. Then, fascicles were assigned to the muscle region that contained the fascicle midpoint and the median muscle fascicle length was calculated for each region. Finally, the mean of all muscle regions was calculated and used as an input for optimal fiber length.

2.2.3. 3D motion capture

3D motion capture (Flex 13, OptiTrack, Corvallis, OR, USA) was used to record a static calibration trial with 8 marker clusters and 16 individual markers placed bilaterally on the lower limbs and pelvis to scale a musculoskeletal model (Rajagopal et al., 2016) for each participant (OpenSim v3.3). Then, during the walking protocol, we used the markers attached bilaterally to the calcaneus and the fifth metatarsophalangeal joint to determine the timing of the heel-strike and toe-off events using custom-written scripts based on foot vertical velocity (O'Connor et al., 2007). Motion capture data were collected at 120 Hz (Motive, OptiTrack, Corvallis, OR, USA) and raw marker positions were filtered using a second-order low-pass Butterworth filter with a cut-off frequency of 10 Hz.

2.2.4. Electromyography

We shaved, abraded and cleaned the participant's skin with alcohol to reduce the skin-electrode impedance. We placed surface electrodes (Trigno Delsys Inc., Natick, USA; 10 mm inter-electrode distance) over the GM and GL muscle bellies, aligned along the direction of the muscle fascicles, determined using B-mode ultrasound. The EMG signals were amplified, digitized at 2048 Hz, band-pass filtered (20-500 Hz), and recorded in Spike2 (V7, CED Ltd, Cambridge, UK). During post-processing, the MVC and walking EMG signals were band-pass filtered using a second-order Butterworth filter (20-500 Hz), rectified, and low-pass filtered at 12 Hz. The maximal value of the EMG signal measured during the MVC trials was considered as the maximal EMG amplitude (EMG_{max}). Then, the EMG signals from 15 gait

cycles were normalized to EMG_{max}. Finally, we interpolated the data from each gait cycle to 100 data points. We averaged all the cycles within a trial and then we averaged the resulting two mean cycles from each trial to finally obtain a single mean cycle for each condition and participant.

2.2.5. B-mode ultrasound

To image the GM and GL during walking, we placed two linear ultrasound probes (5-8 MHz, 60 mm field-of-view, LV8-5L60N-2, ArtUS, Telemed, Vilnius, Lithuania) on the same location as used for the EMG electrodes. The probe orientation was optimized to be aligned in the fascicle plane and secured with elastic bandages. Ultrasound data were recorded at 120 Hz for 15 s of walking. Post data collection, we analyzed five gait cycles of ultrasound data per trial using a validated (Cronin et al., 2011; Gillett et al., 2013) semi-automated tracking algorithm (UltraTrack; Farris and Lichtwark, 2016), combined with manual corrections (for details, see Hamard et al., 2021). Ultrasound data were low-pass filtered at 12 Hz and fascicle velocity was calculated as the first time derivative of fascicle length. We normalized fascicle length to the mean fascicle length at heel-strike during level walking (L_{HS}; average group value: 56.6 ± 8.0 mm and 65.4 ± 10.1 mm for the GM and GL, respectively). Similarly, fascicle velocity was expressed as the normalized fascicle length per second. Ultrasound data from each gait cycle were interpolated to 100 data points and we averaged the cycles within a trial and then between both trials to create a mean cycle for each condition and participant.

2.3. Estimation of time-varying muscle force during walking

We estimated the time-varying forces produced by the GM and GL muscles during walking using a Hill-type model (Zajac, 1989):

$$F_{\mathrm{m}} = F_{\max}\left[\hat{a}(t)\hat{F}_{\mathrm{a}}\left(\hat{l}_{\mathrm{f}}\right)\hat{F}_{\mathrm{a}}(\hat{v}) + \hat{F}_{\mathrm{p}}\left(\hat{l}_{\mathrm{f}}\right)\right]\cos\beta. \quad (1)$$

The muscle force F_{m} (N) was calculated from the maximal force-generating capacity $F_{\max}$, expressed in N, the time-varying normalized activation $\hat{a}(t)$, the normalized active ($\hat{F}_{\mathrm{a}}\left(\hat{l}_{\mathrm{f}}\right)$) and passive ($\hat{F}_{\mathrm{p}}\left(\hat{l}_{\mathrm{f}}\right)$) forces as determined from the force-length relationship, the normalized force $\hat{F}_{\mathrm{a}}(\hat{v})$ as determined from the force-velocity relationship and the cosine of the time-varying pennation angle β (°).

The normalized active force-length curve (Otten, 1987), was modelled as:

$$\hat{F}_{\mathrm{a}}(\hat{l}_{\mathrm{f}}) = e^{-\left(\frac{\hat{l}_{\mathrm{f}}^{0.6}-1}{0.3}\right)^{2.3}}. \quad (2)$$

The normalized passive force-length curve (Otten, 1987) was modelled as:

$$\hat{F}_{\mathrm{p}} = 2.64\hat{l}_{\mathrm{f}}^{\,2} - 5.30\hat{l}_{\mathrm{f}} + 2.66 \quad \text{for} \quad \hat{l}_{\mathrm{f}} > 1, \quad (3)$$

$$\hat{F}_{\mathrm{P}}(\hat{l}_{\mathrm{f}}) = 0 \quad \text{for} \quad \hat{l}_{\mathrm{f}} \leq 1, \quad (4)$$

Where $\hat{l}_{\mathrm{f}}$ is the time-varying normalized fascicle length measured during walking.

The normalized force-velocity curve was modelled as:

$$\hat{F}_{\mathrm{a}}(\hat{v}) = \frac{1+\left(\frac{\hat{v}}{\hat{v}_0}\right)}{1-\left(\frac{\hat{v}}{v_0\alpha}\right)} \quad \text{for} \quad \hat{v} \leq 0, \quad (5)$$

$$\hat{F}_{\mathrm{a}}(\hat{v}) = 1.5 - 0.5\frac{1-\left(\frac{\hat{v}}{\hat{v}_0}\right)}{1+\left(\frac{7.56\hat{v}}{v_0\alpha}\right)} \quad \text{for} \quad \hat{v} > 0, \quad (6)$$

Where $\hat{v}$ is the time-varying normalized fascicle velocity recorded during walking. α describes the curvature of the force velocity relationship and v_0 is the maximum unloaded shortening velocity. We used intermediate values accounting for slow and fast muscle fibers from numerous terrestrial species of 0.235 and -7.5 s^{-1} for α and $\hat{v}_0$, respectively (Wakeling et al., 2012).

Finally, $F_{\max}$ is a function of the muscle's volume Vol, the optimal fiber length $l_{\mathrm{f,opt}}$ and the maximum isometric stress of a muscle fiber σ_0.

$$F_{\max} = \left(\frac{Vol}{l_{\mathrm{f,opt}}}\right)\sigma_0. \quad (7)$$

σ_0 was estimated from the literature (22.5 $N.cm^{-2}$, Powell et al., 1984; Roy et al., 1982; Spector et al., 1980). For the scaling method, $l_{\mathrm{f,opt}}$ was estimated from a subject-specific musculoskeletal model (Delp et al., 2007; Rajagopal et al., 2016). This 37 degrees of freedom model with 97 muscle-tendon complex actuators was scaled to the individual anthropometry of the participants based on the mass of the participant and markers positions recorded during the static trial. For the scaling method, muscle volume was calculated using the regression equations from Handsfield et al. (2014):

$$Vol = b1 \times BM + b2 \quad (8)$$

197 Where Vol (cm^3) is a function of body mass, BM (kg) and two coefficients $b1$ and $b2$.
198 Coefficient $b1$ is 3.41 and 2.19 for the GM and GL, respectively, and $b2$ is 12.60 and -7.59
199 for GM and GL, respectively (Handsfield et al., 2014). Concerning the experimental method,
200 we used, as a substitute for the $l_{f,opt}$, the mean muscle fascicle length estimated from DTI and
201 we used the muscle volume measured from MRI for the GM and GL.

202 **2.4. Statistics**

203 We conducted the statistical analyses in Statistica v8.0 (Statsoft, Tulsa, OK, USA). All data
204 passed the Kolmogorov-Smirnov test for normality. First, we compared the muscle volume,
205 fascicle length and F_{max} between the two methods and the two muscles using 2-way repeated-
206 measures ANOVAs (factor: method [scaling, experimental], muscle [GM, GL]). Additionally,
207 the GM/(GM+GL) ratios of muscle volume, fascicle length and F_{max} were calculated and we
208 used paired t-tests to determine whether these ratios differed between the two methods. We
209 also assessed the relationship between the two estimation methods for muscle volume,
210 fascicle length and F_{max} using Pearson's correlation coefficient. Finally, we used the root
211 mean square error (RMSE) to determine the discrepancy between methods for muscle volume,
212 fascicle length and F_{max}.

213 From the predicted force output, we extracted the peak force, corresponding to the maximal
214 force value during the gait cycle and the force integral, corresponding to the integral of the
215 time-varying force. To test our first hypothesis, we used 3-way repeated-measures ANOVAs
216 (factor: method [scaling, experimental], muscle [GM, GL] and condition [level, incline]) to
217 determine whether the peak force or the force integral systematically differed between
218 methods, muscles or conditions. Then, the GM/(GM+GL) ratios for peak force and force
219 integral were calculated to estimate the force-sharing strategy between the gastrocnemii. We
220 performed 2-way repeated-measures ANOVAs (factor: method [scaling, experimental] and
221 condition [level, incline]) on these ratios to assess whether they systematically differed
222 between methods and between conditions. Finally, we compared the peak force and force
223 integral between the two methods using the RMSE. For all tests, the level of significance was
224 set at $P<0.05$.

3. RESULTS

3.1. Maximal force-generating capacity

Fig. 1 depicts the results for volume, fascicle length and F_{max}. This paragraph, however, presents only the results for F_{max} as they are more closely related to our aim. There was a main effect of muscle (P<0.001) on F_{max}, with no main effect of method (P=0.744), nor a muscle × method interaction (P=0.265). Specifically, the GM had a larger F_{max} (1072 ± 240 N) than the GL (587 ± 166 N) regardless of the method. Moreover, the correlation between F_{max} estimated from the scaling method and F_{max} estimated from experimental data was strong for both the GM (R=0.871; P<0.001) and the GL (R=0.739; P=0.006). Even though there was no statistical difference in the GM/(GM+GL) ratio of F_{max} between the methods (66.5 ± 0.5% for the scaling method and 63.0 ± 5.6% for the experimental method; P=0.056), inspection of individual data indicated large differences between methods for some participants, with the difference being up to 12.5% (Fig. 1). We found high RMSE values between methods for the F_{max}, i.e. 186 N for the GM and 160 N for the GL corresponding to 18.1% and 26.3% of the average F_{max}, respectively. Moreover, a discrepancy between calculation methods for F_{max} was also observed for the GM/(GM+GL) ratios as indicated by a RMSE of 6.5%.

3.2. Force output

When considering the peak force, which occurred during the stance phase (Fig. 2), there was a main effect of muscle (P<0.001) and condition (P=0.001), with no main effect of method (P=0.513), nor any interaction (all P≥0.303) (Table 1). Similarly, when considering the force integral calculated over the whole gait cycle, we observed a main effect of muscle (P<0.001) and condition (P=0.003), with no main effect of method (P=0.557), nor any interaction (all P≥0.333). Overall, the GM produced more force compared to the GL during walking (+170 ± 96% and +159 ± 100% for peak force and force integral, respectively), regardless of the method. In addition, higher peak force (+34 ± 18%) and force integral (+27 ± 14%) were predicted during incline walking compared to level walking, regardless of the muscle and method.

When considering the peak force ratio (i.e. the force-sharing strategy between muscles), there was a main effect of condition (P=0.046), with no main effect of method (P=0.163) or a method × condition interaction (P=0.984). Specifically, the ratio of peak force was lower (closer to 50%) during incline walking compared to level walking (Table 2). When

considering the ratio of the force integral, there was no main effect of method (P=0.137), nor an effect of condition (P=0.071) or a method × condition interaction (P=0.971).

Even though the group data did not exhibit significant differences between methods, inspection of Fig. 2 and 3 revealed noteworthy differences between methods for some participants. The difference in model-predicted forces between the methods was greater than 30% for four participants for GM and for three participants for GL during level walking. When considering the ratios (i.e. the force-sharing strategy between muscles), similar observations were made, i.e. despite the between-methods difference being lower than 1% in four participants for both peak force and force integral, the between-methods difference was substantial (greater than 6%) for four participants. These individual differences led to relatively high RMSE group values. When considering the peak force during level walking, the RMSE between the two methods was 66 N for the GM and 28 N for the GL corresponding to 19.0% and 22.1% of the group-averaged peak force, respectively. We also found high RMSE values for the force integral, i.e. 20 N.s for the GM and 12 N.s for the GL corresponding to 18.0% and 25.9% of the average force integral, respectively. Moreover, discrepancy between methods was also observed for the GM/(GM+GL) ratios of peak force and force integral. The RMSE between methods was 5.4% for peak force and 5.7% for the force integral in level walking.

4. DISCUSSION

We determined the influence of two different personalization methods on a Hill-type model's predicted force-sharing strategy between the gastrocnemii during walking. We found substantial differences between the scaling method and the experimental method in the predicted force-sharing strategies at the individual level. Therefore, generic scaling methods may be unable to estimate the force-sharing strategy at the level of individual participants.

Our main results indicate substantial differences between methods for some participants. This is consistent with previous studies, which highlight that inclusion of subject-specific musculoskeletal geometry (Wesseling et al., 2016) or muscle-tendon origin and insertion (Bosmans et al., 2015) affects a model's force estimation. Furthermore, our results are similar to previous studies that report high inter-individual variability in the distribution of maximal force-generating capacity between synergist muscles from either the triceps surae (Crouzier et al., 2018) or the quadriceps (Hug et al., 2015). However, here we also highlight that the force-sharing strategy varies markedly between individuals during walking - a dynamic task whereby forces are submaximal. Furthermore, during walking, a substantial difference between the scaling method and the experimental method (> 6%) for GM/(GM+GL) ratio of either peak force or the force integral was observed in one third of the participants. Similar levels of differences in the GM/(GM+GL) ratio (+6-10%) were shown in patients with Achilles tendinopathy compared to asymptomatic individuals during submaximal isometric contractions (Crouzier et al., 2019). It is therefore possible that the use of generic scaling methods may reduce the ability to detect pathological force-sharing strategies for individuals who deviate from the generic maximal force-generating capacity distribution, which is often the case in clinical populations (Barber et al., 2011).

We compared model-predicted forces when using two different methods to estimate a muscle's maximal force-generating capacity. However, an inherent limitation of such an approach is the inability to evaluate our model against direct measurements of *in vivo* force. We compared our predicted forces with forces previously estimated or measured using different approaches during similar walking conditions. For the GM, we found similar peak force levels (346 N) to those estimated using inverse dynamics analysis combined with moment arm and PCSA calculations (~305 N in Farris and Sawicki, 2012). In addition, our predicted forces are in agreement with tendon forces directly measured *in vivo*. Finni et al. (1998) reported a peak Achilles tendon force of 1320 N for the triceps surae during an

analogous walking speed (1.1 $m.s^{-1}$). Similar to previous methods (Dick et al., 2016), we combined this peak force with the relative PCSA of the gastrocnemii within the triceps surae (~26% for the GM and 12% for the GL; Ward et al., 2009) and accounted for the relative gastrocnemii activation levels during walking relative to the triceps surae (~40% MG, 20% LG; Crouzier et al., 2019) to calculate a peak force of 365 N for the GM and 84 N for the GL – which is consistent with our predicted forces (346 N for the GM and 128 N for the GL for the experimental method).

Although our results revealed no difference between methods at the group level, this result is difficult to generalize to other groups such as clinical populations. Moreover, we found a similar estimation of muscle volume for group averages when using a scaling method (Handsfield et al., 2014) versus MRI-derived muscle volumes (Fig. 1A) but, on the other hand, the estimation of fascicle length varied more between the scaling and DTI methods (Fig. 1B). This is likely because the scaling method uses subject-specific musculoskeletal models that provide the theoretical optimal fiber length based on a constant muscle-tendon geometry across all participants, whereas the DTI method provides the resting fascicle length at 90° of plantarflexion and < 5° of knee flexion, which accounts for individual differences in resting fascicle lengths. Despite personalizing the maximal force-generating capacity, activation, fascicle length and velocity, and pennation angle, some model parameters remained generic. For example, the shape of the force-length and force-velocity relationships were consistent across models and individuals whereas the inter-individual variability in these relationships has been suggested in human GM (Hager et al., 2020) and vastus lateralis muscles (Brennan et al., 2018). However, the influence of these parameters on predicted forces is likely small given the relatively low sensitivity of Hill-type models to, for example, the curvature of the force-velocity relationship and the maximum unloaded shortening velocity (Dick et al., 2017). On the other hand, previous studies have shown that the Hill-type model is also sensitive to tendon slack length and optimal fiber length (Bujalski et al., 2018; Scovil & Ronsky, 2006). Further work is needed to test the effect of personalising these parameters on muscle force estimation, although directly measuring these parameters in humans *in vivo* is currently not possible.

In conclusion, when predicting individual muscle force-sharing strategies, our results highlight the importance for Hill-type models to be personalized with *in vivo* imaging data. Future research is necessary to determine the sensitivity of Hill-type models to additional

subject-specific inputs, for example by using elastography to estimate the fascicle slack length and the muscle's passive force-length properties (Hug et al., 2013) or by estimating subject-specific force-length relationships (Maganaris, 2003).

Acknowledgements:

We thank Aiman Al-Najjar, Nicole Atcheson, and Donald Maillet from the UQ Centre for Advanced Imaging (CAI) for their support and expertise in MR imaging. We further thank Bart Bolsterlee (NeuRA & University of New-South Wales) for assistance in MRI and DTI processing.

Declaration of competing interest

The authors in this paper have no financial or other relationships that might lead to a conflict of interest.

Funding

This work was supported by a University of Queensland Early Career Research Grant to Taylor JM Dick. François Hug is supported by a fellowship from the Institut Universitaire de France (IUF) and a travel grant from the Société de Biomécanique. Support was received from the French national research agency (ANR-19-CE17-002, COMMODE project; to FH).

Data availability:

The predicted force data are available from figshare: 10.6084/m9.figshare.17099864

REFERENCES

Aeles, J., Bolsterlee, B., Kelp, N. Y., Dick, T. J. M., & Hug, F. (2021). Regional variation in lateral and medial gastrocnemius muscle fibre lengths obtained from diffusion tensor imaging. *Journal of Anatomy*. https://doi.org/10.1111/joa.13539

Barber, L., Barrett, R., & Lichtwark, G. (2011). Passive muscle mechanical properties of the medial gastrocnemius in young adults with spastic cerebral palsy. *Journal of Biomechanics*, *44*(13), 2496-2500. https://doi.org/10.1016/j.jbiomech.2011.06.008

Bolsterlee. (2020). *GitHub—Bartbols/SASHIMI: SASHIMI segmentation is a Matlab App for semi-automatic interactive segmentation of multi-slice images.* https://github.com/bartbols/SASHIMI

Bosmans, L., Valente, G., Wesseling, M., Van Campen, A., De Groote, F., De Schutter, J., & Jonkers, I. (2015). Sensitivity of predicted muscle forces during gait to anatomical variability in musculotendon geometry. *Journal of Biomechanics*, *48*(10), 2116-2123. https://doi.org/10.1016/j.jbiomech.2015.02.052

Brennan, S. F., Cresswell, A. G., Farris, D. J., & Lichtwark, G. A. (2018). The effect of muscle-tendon unit vs. Fascicle analyses on vastus lateralis force-generating capacity during constant power output cycling with variable cadence. *Journal of Applied Physiology*, *124*(4), 993-1002. https://doi.org/10.1152/japplphysiol.00356.2017

Bujalski, P., Martins, J., & Stirling, L. (2018). A Monte Carlo analysis of muscle force estimation sensitivity to muscle-tendon properties using a Hill-based muscle model. *Journal of Biomechanics*, *79*, 67-77. https://doi.org/10.1016/j.jbiomech.2018.07.045

Cronin, N. J., Carty, C. P., Barrett, R. S., & Lichtwark, G. (2011). Automatic tracking of medial gastrocnemius fascicle length during human locomotion. *Journal of Applied Physiology (Bethesda, Md.: 1985)*, *111*(5), 1491-1496. https://doi.org/10.1152/japplphysiol.00530.2011

Crouzier, M., Hug, F., Dorel, S., Deschamps, T., Tucker, K., & Lacourpaille, L. (2019). Do individual differences in the distribution of activation between synergist muscles reflect individual strategies? *Experimental Brain Research*, *237*(3), 625-635. https://doi.org/10.1007/s00221-018-5445-6

Crouzier, M., Lacourpaille, L., Nordez, A., Tucker, K., & Hug, F. (2018). Neuromechanical coupling within the human triceps surae and its consequence on individual force-sharing strategies. *The Journal of Experimental Biology*, *221*(21), jeb187260. https://doi.org/10.1242/jeb.187260

Crouzier, M., Tucker, K., Lacourpaille, L., Doguet, V., Fayet, G., Dauty, M., & Hug, F. (2019). Force-sharing within the Triceps Surae : An Achilles Heel in Achilles Tendinopathy. *Medicine & Science in Sports & Exercise*, *Publish Ahead of Print*. https://doi.org/10.1249/MSS.0000000000002229

Dal, U., Erdogan, T., Resitoglu, B., & Beydagi, H. (2010). Determination of preferred walking speed on treadmill may lead to high oxygen cost on treadmill walking. *Gait & Posture*, *31*(3), 366-369. https://doi.org/10.1016/j.gaitpost.2010.01.006

Delp, S. L., Anderson, F. C., Arnold, A. S., Loan, P., Habib, A., John, C. T., Guendelman, E., & Thelen, D. G. (2007). OpenSim : Open-source software to create and analyze dynamic simulations of movement. *IEEE Transactions on Bio-Medical Engineering*, *54*(11), 1940-1950. https://doi.org/10.1109/TBME.2007.901024

Dick, T. J. M., Biewener, A. A., & Wakeling, J. M. (2017). Comparison of human gastrocnemius forces predicted by Hill-type muscle models and estimated from ultrasound images. *The Journal of Experimental Biology*, *220*(9), 1643-1653. https://doi.org/10.1242/jeb.154807

Dick, T. JM., Arnold, A. S., & Wakeling, J. M. (2016). Quantifying Achilles Tendon Force In Vivo from Ultrasound Images. *Journal of biomechanics*, *49*(14), 3200-3207. https://doi.org/10.1016/j.jbiomech.2016.07.036

Farris, D. J., & Lichtwark, G. A. (2016). UltraTrack : Software for semi-automated tracking of muscle fascicles in sequences of B-mode ultrasound images. *Computer Methods and Programs in Biomedicine*, *128*, 111-118. https://doi.org/10.1016/j.cmpb.2016.02.016

Farris, D. J., & Sawicki, G. S. (2012). Human medial gastrocnemius force-velocity behavior shifts with locomotion speed and gait. *Proceedings of the National Academy of Sciences of the United States of America*, *109*(3), 977-982. https://doi.org/10.1073/pnas.1107972109

Finni, T., Komi, P. V., & Lukkariniemi, J. (1998). Achilles tendon loading during walking : Application of a novel optic fiber technique. *European Journal of Applied Physiology and Occupational Physiology*, *77*(3), 289-291. https://doi.org/10.1007/s004210050335

Gillett, J. G., Barrett, R. S., & Lichtwark, G. A. (2013). Reliability and accuracy of an automated tracking algorithm to measure controlled passive and active muscle fascicle length changes from ultrasound. *Computer Methods in Biomechanics and Biomedical Engineering*, *16*(6), 678-687. https://doi.org/10.1080/10255842.2011.633516

Gregor, R. J., Komi, P. V., & Järvinen, M. (1987). Achilles Tendon Forces During Cycling. *International Journal of Sports Medicine*, *08*(S 1), S9-S14. https://doi.org/10.1055/s-2008-1025698

Hager, R., Poulard, T., Nordez, A., Dorel, S., & Guilhem, G. (2020). Influence of joint angle on muscle fascicle dynamics and rate of torque development during isometric explosive contractions. *Journal of Applied Physiology*, *129*(3), 569-579. https://doi.org/10.1152/japplphysiol.00143.2019

Hamard, R., Aeles, J., Kelp, N. Y., Feigean, R., Hug, F., & Dick, T. J. M. (2021). Does different activation between the medial and the lateral gastrocnemius during walking translate into different fascicle behavior? *The Journal of Experimental Biology*, *224*(12), jeb242626. https://doi.org/10.1242/jeb.242626

Handsfield, G. G., Meyer, C. H., Hart, J. M., Abel, M. F., & Blemker, S. S. (2014). Relationships of 35 lower limb muscles to height and body mass quantified using MRI. *Journal of Biomechanics*, *47*(3), 631-638. https://doi.org/10.1016/j.jbiomech.2013.12.002

Hug, F., Goupille, C., Baum, D., Raiteri, B. J., Hodges, P. W., & Tucker, K. (2015). Nature of the coupling between neural drive and force-generating capacity in the human quadriceps muscle. *Proceedings. Biological Sciences*, *282*(1819). https://doi.org/10.1098/rspb.2015.1908

Hug, F., Lacourpaille, L., Maïsetti, O., & Nordez, A. (2013). Slack length of gastrocnemius medialis and Achilles tendon occurs at different ankle angles. *Journal of Biomechanics*, *46*(14), 2534-2538. https://doi.org/10.1016/j.jbiomech.2013.07.015

Hug, F., & Tucker, K. (2017). Muscle Coordination and the Development of Musculoskeletal Disorders. *Exercise and Sport Sciences Reviews*, *45*(4), 201-208. https://doi.org/10.1249/JES.0000000000000122

Komi, P. V. (1990). Relevance of in vivo force measurements to human biomechanics. *Journal of Biomechanics*, *23*, 23-34. https://doi.org/10.1016/0021-9290(90)90038-5

Maganaris, C. N. (2003). Force-length characteristics of the in vivo human gastrocnemius muscle. *Clinical Anatomy*, *16*(3), 215-223. https://doi.org/10.1002/ca.10064

Millard, M., Uchida, T., Seth, A., & Delp, S. L. (2013). Flexing Computational Muscle : Modeling and Simulation of Musculotendon Dynamics. *Journal of Biomechanical Engineering*, *135*(2). https://doi.org/10.1115/1.4023390

O'Connor, C. M., Thorpe, S. K., O'Malley, M. J., & Vaughan, C. L. (2007). Automatic detection of gait events using kinematic data. *Gait & Posture*, *25*(3), 469-474. https://doi.org/10.1016/j.gaitpost.2006.05.016

Otten, E. (1987). A myocybernetic model of the jaw system of the rat. *Journal of Neuroscience Methods*, *21*(2), 287-302. https://doi.org/10.1016/0165-0270(87)90123-3

Perreault, E. J., Heckman, C. J., & Sandercock, T. G. (2003). Hill muscle model errors during movement are greatest within the physiologically relevant range of motor unit firing rates. *Journal of Biomechanics*, *36*(2), 211-218. https://doi.org/10.1016/s0021-9290(02)00332-9

Pinel, S., Kelp, N. Y., Bugeja, J. M., Bolsterlee, B., Hug, F., & Dick, T. J. M. (2021). Quantity versus quality : Age-related differences in muscle volume, intramuscular fat, and mechanical properties in the triceps surae. *Experimental Gerontology*, *156*, 111594. https://doi.org/10.1016/j.exger.2021.111594

Powell, P. L., Roy, R. R., Kanim, P., Bello, M. A., & Edgerton, V. R. (1984). Predictability of skeletal muscle tension from architectural determinations in guinea pig hindlimbs. *Journal of Applied Physiology*, *57*(6), 1715-1721. https://doi.org/10.1152/jappl.1984.57.6.1715

Rajagopal, A., Dembia, C. L., DeMers, M. S., Delp, D. D., Hicks, J. L., & Delp, S. L. (2016). Full-Body Musculoskeletal Model for Muscle-Driven Simulation of Human Gait. *IEEE Transactions on Biomedical Engineering*, *63*(10), 2068-2079. https://doi.org/10.1109/TBME.2016.2586891

Roy, R. R., Meadows, I. D., Baldwin, K. M., & Edgerton, V. R. (1982). Functional significance of compensatory overloaded rat fast muscle. *Journal of Applied Physiology*, *52*(2), 473-478. https://doi.org/10.1152/jappl.1982.52.2.473

Scovil, C. Y., & Ronsky, J. L. (2006). Sensitivity of a Hill-based muscle model to perturbations in model parameters. *Journal of Biomechanics*, *39*(11), 2055-2063. https://doi.org/10.1016/j.jbiomech.2005.06.005

Spector, S. A., Gardiner, P. F., Zernicke, R. F., Roy, R. R., & Edgerton, V. R. (1980). Muscle architecture and force-velocity characteristics of cat soleus and medial gastrocnemius : Implications for motor control. *Journal of Neurophysiology*, *44*(5), 951-960. https://doi.org/10.1152/jn.1980.44.5.951

Wakeling, J. M., Lee, S. S. M., Arnold, A. S., de Boef Miara, M., & Biewener, A. A. (2012). A Muscle's Force Depends on the Recruitment Patterns of Its Fibers. *Annals of Biomedical Engineering*, *40*(8), 1708-1720. https://doi.org/10.1007/s10439-012-0531-6

Ward, S. R., Eng, C. M., Smallwood, L. H., & Lieber, R. L. (2009). Are Current Measurements of Lower Extremity Muscle Architecture Accurate? *Clinical Orthopaedics and Related Research*, *467*(4), 1074-1082. https://doi.org/10.1007/s11999-008-0594-8

Wesseling, M., De Groote, F., Bosmans, L., Bartels, W., Meyer, C., Desloovere, K., & Jonkers, I. (2016). Subject-specific geometrical detail rather than cost function formulation affects hip loading calculation. *Computer Methods in Biomechanics and Biomedical Engineering*, *19*(14), 1475-1488. https://doi.org/10.1080/10255842.2016.1154547

Zajac, F. E. (1989). Muscle and tendon : Properties, models, scaling, and application to biomechanics and motor control. *Critical Reviews in Biomedical Engineering*, *17*(4), 359-411.

TABLES AND FIGURES

Table 1: Force parameters estimated using the Hill-type model during level and incline walking.

	Level walking				Incline walking			
	GM		GL		GM		GL	
	Scaling	Experimental	Scaling	Experimental	Scaling	Experimental	Scaling	Experimental
Peak force (N)	378 ± 127	346 ± 137	120 ± 41*	128 ± 55*	467 ± 152†	423 ± 155†	186 ± 64*†	195 ± 74*†
Force integral (N.s)	123 ± 36	114 ± 43	43 ± 15*	45 ± 17*	149 ± 48†	136 ± 52†	61 ± 21*†	65 ± 26*†

Values are presented for the gastrocnemius medialis and lateralis during both level and incline walking. The maximal force-generating capacity was estimated using either the scaling or experimental method. GM, gastrocnemius medialis, GL, gastrocnemius lateralis. Values are reported as mean ± standard deviation. *Indicates a significant difference with GM. †Indicates a significant difference with level walking. n = 12. No difference between methods was found for any muscle or condition.

Table 2: Gastrocnemius medialis to gastrocnemius lateralis [GM/(GM+GL)] force ratio estimated using the Hill-type model during level and incline walking.

	Level walking		Incline walking	
	Scaling method	Experimental method	Scaling method	Experimental method
Peak force ratio (%)	75.4 ± 6.2	72.4 ± 7.3	71.1 ± 7.8†	68.0 ± 7.9†
Force integral ratio (%)	74.1 ± 6.2	71.2 ± 7.3	70.5 ± 7.0	67.4 ± 7.5

Values are presented for both level and incline walking. The maximal force-generating capacity was estimated using either a scaling or experimental method. Values are reported as mean ± standard deviation. †Indicates significant difference with level walking. n = 12. No difference between methods was found for any muscle or condition.

FIGURE LEGENDS

Fig. 1: Individual data for muscle volume (A), fascicle length (B) and maximal force-generating capacity (F_{max}; C) determined using the scaling and experimental methods. Data are depicted for both the gastrocnemius medialis (GM) and gastrocnemius lateralis (GL). The ratio between these muscles [GM/(GM+GL)] is also depicted for each variable. Each graph depicts individual data obtained with the scaling method (top) and experimental method (bottom). Each color represents an individual participant and the mean group value is presented as a black diamond. Because the scaling method uses the same underlying equations to scale all individuals, we can observe that the inter-individual variability in ratios between muscles is concealed.

Fig. 2: Individual time-varying forces estimated by the Hill-type model during level walking for each participant (P). The GM (green) and GL (purple) forces are depicted by solid lines (experimental method) and dashed lines (scaling method). Heel-strike occurred at 0% on the x-axis and the dashed vertical lines represent the timing of toe-off during the gait cycle. Each plot represents an individual participant. Predicted forces for incline walking are presented in Fig. S1.

Fig. 3: Individual data for peak force (A and B) and force integral (C and D) for level walking (white area; A and C) and incline walking (grey area; B and D), determined using the scaling and experimental methods. Data are depicted for both the gastrocnemius medialis (GM) and gastrocnemius lateralis (GL). The ratio [GM/(GM+GL)] is also depicted for each variable. Each graph depicts individual data obtained with the scaling method and experimental method. Each color represents an individual participant and the mean group value is presented as a black diamond. The scaling method and the experimental method seem to predict similar muscle force and force-sharing strategy during walking at the group level but substantial differences between methods was apparent for some participants.

SUPPLEMENTARY FIGURE

Fig. S1: Individual time-varying forces estimated by the Hill-type model during incline walking for each participant (P). *The GM (green) and GL (purple) forces are depicted by solid lines (experimental method) and dashed lines (scaling method). Heel-strike occurred at 0% on the x-axis and the dashed vertical lines represent the timing of toe-off during the gait cycle. Each plot represents an individual participant.*

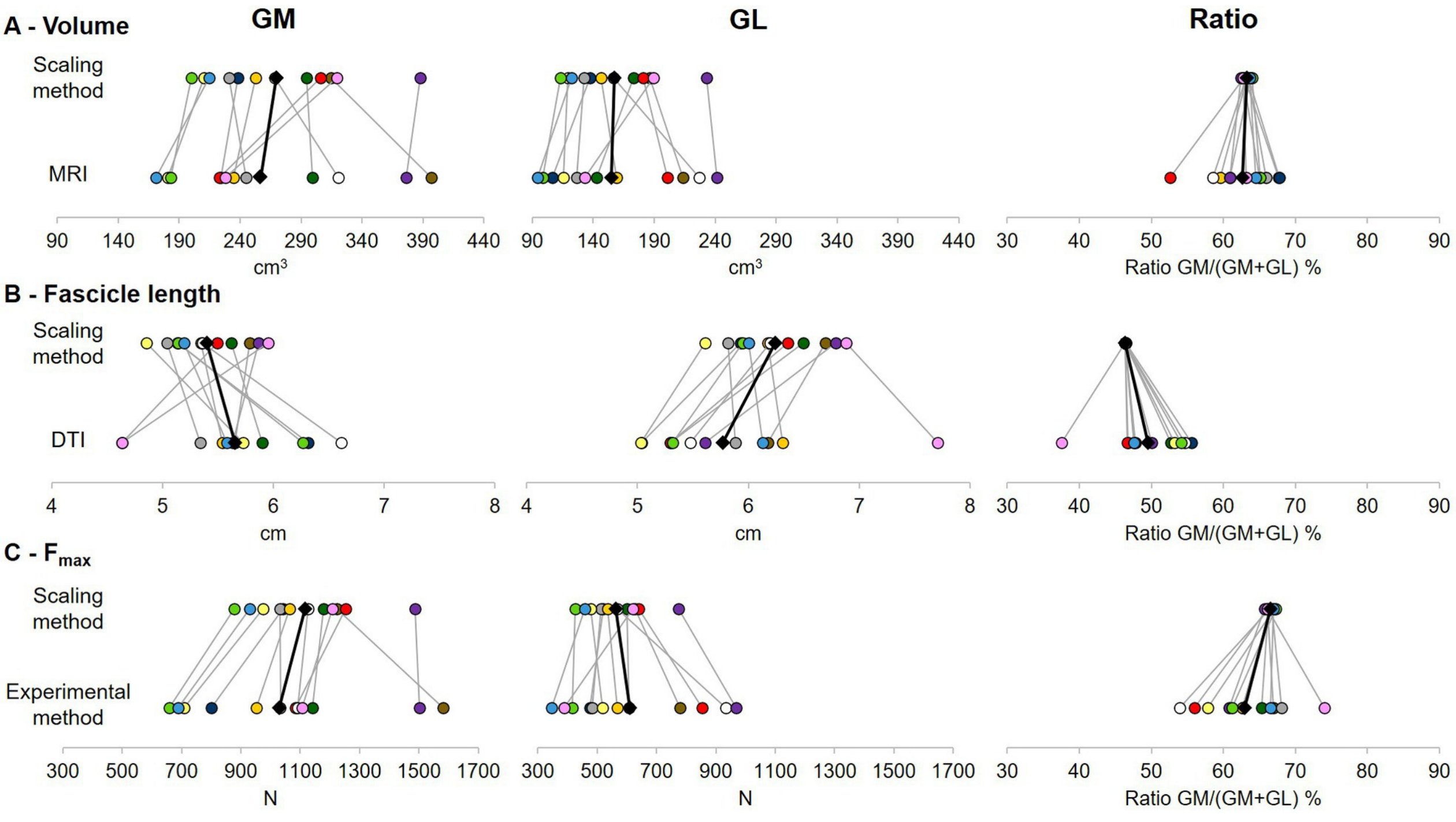
A - Volume
GM
GL
Ratio
Scaling method
MRI
90 140 190 240 290 340 390 440
cm³
90 140 190 240 290 340 390 440
cm³
30 40 50 60 70 80 90
Ratio GM/(GM+GL) %
B - Fascicle length
Scaling method
DTI
4 5 6 7 8
cm
4 5 6 7 8
cm
30 40 50 60 70 80 90
Ratio GM/(GM+GL) %
C - F max
Scaling method
Experimental method
300 500 700 900 1100 1300 1500 1700
N
300 500 700 900 1100 1300 1500 1700
N
30 40 50 60 70 80 90
Ratio GM/(GM+GL) %

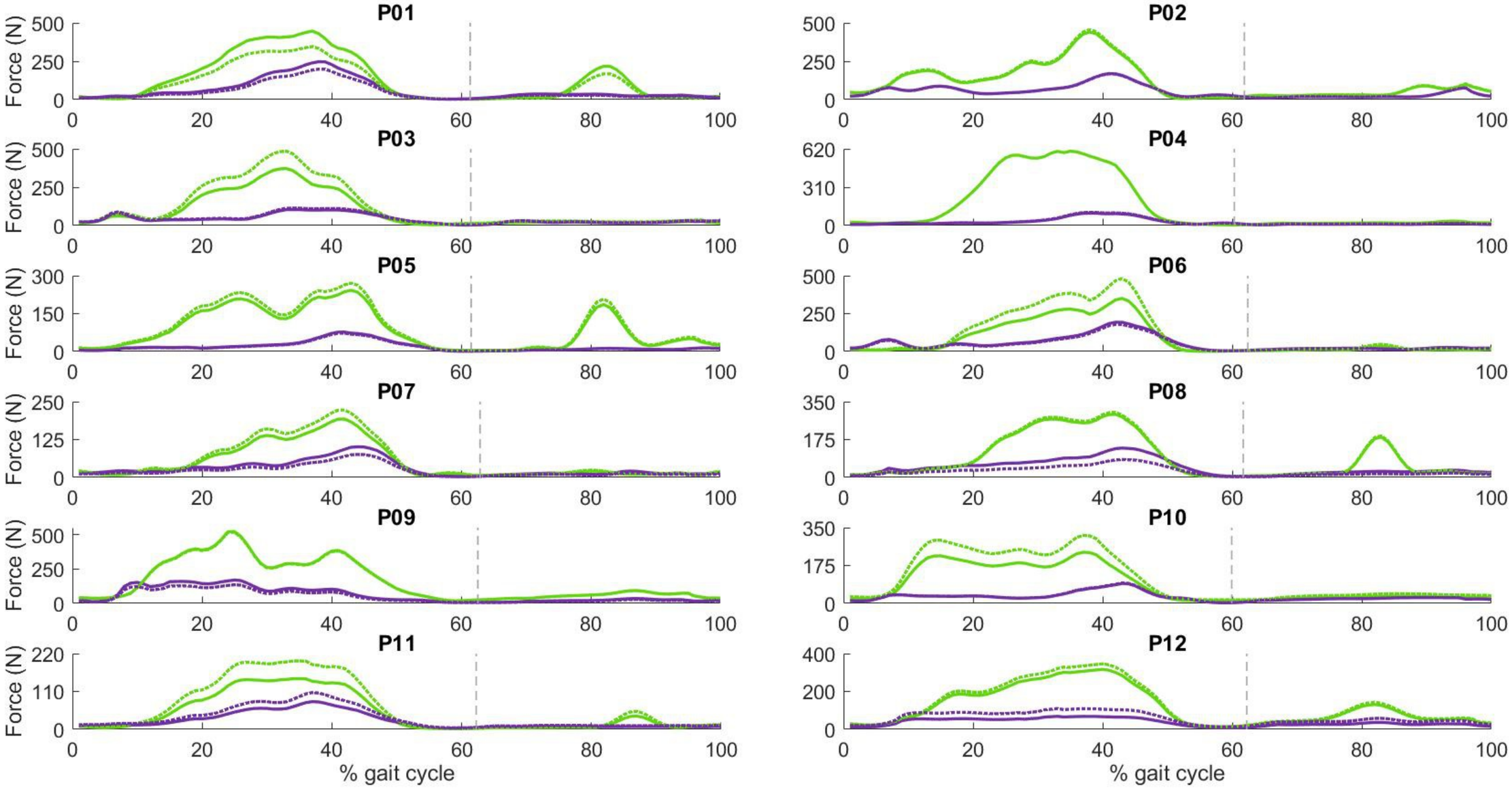
P01
P02
P03
P04
P05
P06
P07
P08
P09
P10
P11
P12
Force (N)
% gait cycle
GM experimental method
GL experimental method
GM scaling method
GL scaling method

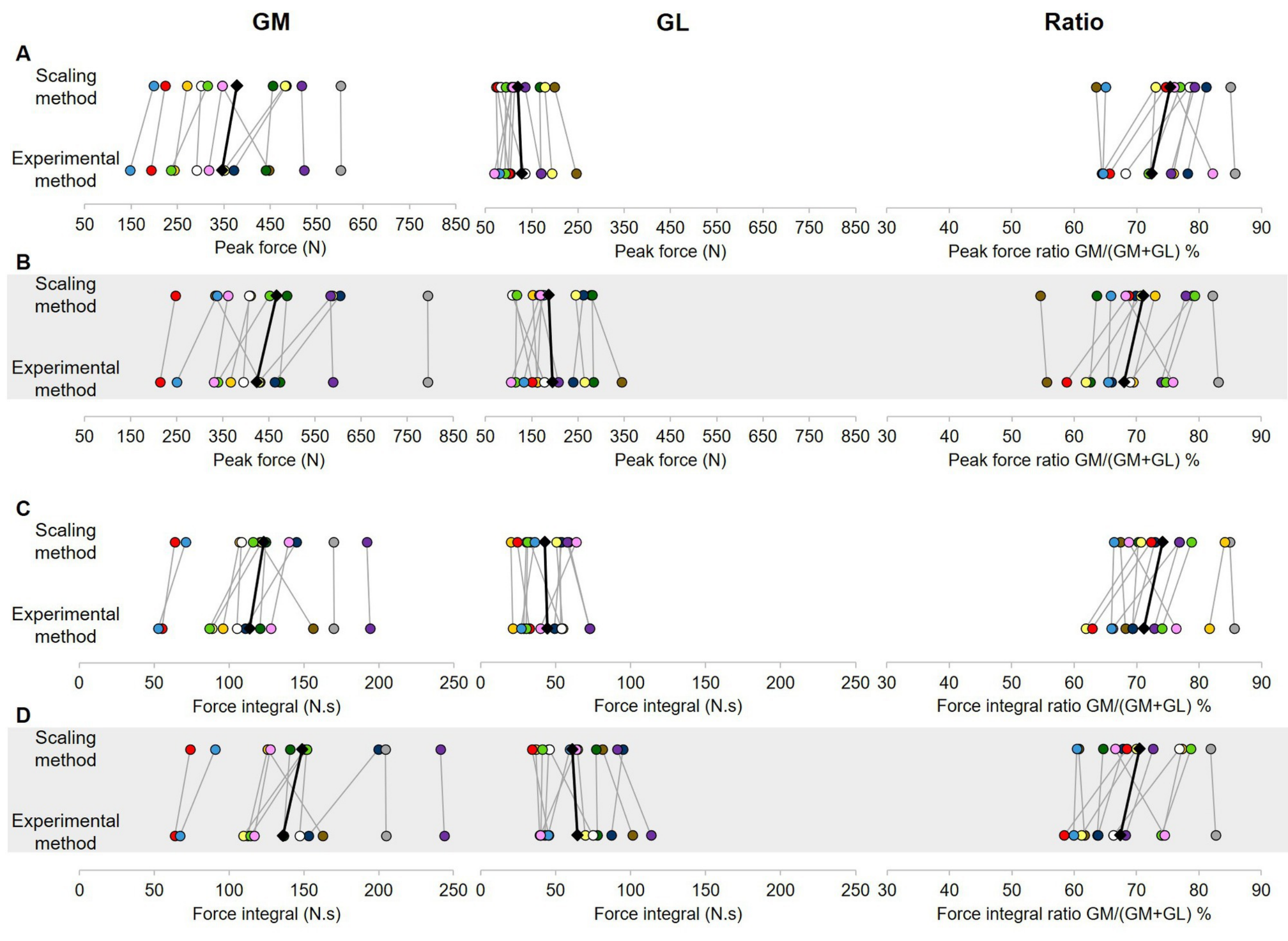
GM
GL
Ratio
A
Scaling method
Experimental method
50 150 250 350 450 550 650 750 850
Peak force (N)
50 150 250 350 450 550 650 750 850
Peak force (N)
30 40 50 60 70 80 90
Peak force ratio GM/(GM+GL) %
B
Scaling method
Experimental method
50 150 250 350 450 550 650 750 850
Peak force (N)
50 150 250 350 450 550 650 750 850
Peak force (N)
30 40 50 60 70 80 90
Peak force ratio GM/(GM+GL) %
C
Scaling method
Experimental method
0 50 100 150 200 250
Force integral (N.s)
0 50 100 150 200 250
Force integral (N.s)
30 40 50 60 70 80 90
Force integral ratio GM/(GM+GL) %
D
Scaling method
Experimental method
0 50 100 150 200 250
Force integral (N.s)
0 50 100 150 200 250
Force integral (N.s)
30 40 50 60 70 80 90
Force integral ratio GM/(GM+GL) %